JOURNAL OF CATALYSIS 119, 277–287 (1989)

Structural, Surface, and Catalytic Properties of Bismuth Molybdovanadates Containing Foreign Atoms

IV. Surface Characterization and Redox Behaviour of Iron-Containing Bismuth Molybdovanadate Catalysts by X-Ray Photoelectron Spectroscopy

D. GAZZOLI,[1] A. ANICHINI, S. DE ROSSI, M. INVERSI, M. LO JACONO, P. PORTA, AND M. VALIGI

Centro SACSO CNR, Dipartimento di Chimica, Università "La Sapienza," Piazzale Aldo Moro 5, 00185 Roma, Italy

Received November 22, 1988; revised March 17, 1989

X-ray photoelectron spectroscopy has been applied to the study of the surface composition and the redox behaviour of multicomponent oxide catalysts having the scheelite structure and general formula $Bi_{1-x/3}\square_{x/3-y}Me_y(V_{1-x}Mo_{x-y}Fe_y)O_4$ (Me = Fe or Bi, $\square$ = cation vacancies), before and after exposure to hydrogen, propene, and a propene + oxygen mixture. The results point to a different reactivity toward the various reactants. By interaction with hydrogen, an extensive reduction is obtained with considerable change of the catalyst surface composition. The reduction behaviour depends on the sample composition, the iron-containing catalysts being reduced at low temperature (140°C). As regards propene treatment, a preferential reactivity of bismuth with propene has been found, regardless of the sample composition. Bismuth is reduced at low temperature (175°C) with ensuing migration to the surface. Under conditions leading to the catalytic oxidation of propene, a high surface stability is exhibited by these compounds. The catalysts remain oxidized and the surface composition reflects that of the bulk. A correlation with the catalytic properties has also been made on the basis of the different mobility of the oxygen ions among the samples examined.

INTRODUCTION

The catalytic properties of systems based on bismuth molybdates for the (ammo)oxidation of olefins have been extensively studied (*1*). However, despite the many papers devoted to the oxidative conversion of olefins and despite a general agreement upon the stages, such as initial olefin chemisorption, α-hydrogen abstraction, and allyl intermediate formation, the role of the individual components of the catalysts in the various reaction steps is a current controversy (*2–4*). In order to obtain further insight into the properties of these systems, a study of a new class of catalysts with scheelite structure and general formula $Bi_{1-x/3}\square_{x/3-y}Me_y(V_{1-x}Mo_{x-y}Fe_y)O_4$ (Me = Fe or Bi, $\square$ = cation vacancies) has been undertaken in our laboratory. Detailed studies concerning the sample preparation, structural characterization, and catalytic properties have already been reported (*5–7*).

In the present work, X-ray photoelectron spectroscopy (XPS) has been applied to study the surface properties and the redox behaviour of such compounds before and after interaction with hydrogen and propene (directly in the high-pressure preparation chamber of the instrument), and a propene + oxygen mixture, with the aim of clarifying the intermediate steps and the transformations which occur on the catalyst surface under reaction conditions.

EXPERIMENTAL

Sample Preparation and Characterization

The catalysts were prepared by a coprecipitation method and final calcination at

[1] To whom correspondence should be addressed.

0021-9517/89 $3.00

600°C in air for 24 h. Details of the sample preparation and characterization are given elsewhere (*5*). As already described in detail (*5*), these compounds have the scheelite structure and general formula $Bi_{1-x/3}\square_{x/3-y}Me_y(V_{1-x}Mo_{x-y}Fe_y)O_4$ (Me = Fe or Bi, □ = cation vacancy). According to the general formula, three series of samples were prepared: (i) iron-free samples ($y = 0.00$) in which Mo^{6+} replace V^{5+} ions in the tetrahedral sites of the high-temperature $BiVO_4$ scheelite structure, whereas cation vacancies and bismuth are located in the eight-coordinated sites of the structure; (ii) iron-containing samples (Me = Fe) derived from bismuth molybdovanadates, where Fe^{3+} ions partly substitute molybdenum in tetrahedral sites and partly fill an equivalent amount of eight-coordinated cation vacancies; and (iii) iron-containing samples (Me = Bi) in which Fe^{3+} ions interchange with Mo^{6+} ions in tetrahedral sites and Bi^{3+} ions fill an equivalent amount of cation vacancies.

The compositions of the samples investigated are reported in Table 1.

XPS Measurements and Sample Treatments

The spectra were recorded with a Leybold–Heraeus LHS 10 spectrometer operating in FAT mode, using a twin Al$K\alpha$ (1486.6 eV; 12 kV, 10 mA) and Mg$K\alpha$ (1253.6 eV; 10 kV, 20 mA) anode and interfaced to a 2113B HP computer. The samples, made into fine powder, were pressed onto a gold-decorated tantalum plate attached to the sample holder. The samples were treated in air at 600°C for 3 h before mounting for XPS.

Reduction of the samples in pure flowing H_2 or propene was carried out directly in the XPS high-pressure preparation chamber in the temperature range 90°–360°C, for 30 min. The treatment temperatures refer to the effective sample temperature monitored by a thermocouple contacting the sample surface. After being cooled gradually to room temperature in an H_2 or propene stream, the sample probe was pushed into the analysis chamber. The latter was evacuated to better than 10^{-9} Torr (1 Torr = 133.3 N m^{-2}) during scans.

Treatments in the reacting mixture $C_3H_6:O_2:He$ (20:20:60 %vol) were performed in a flow reactor in the temperature range 200°–450°C for 30 min, using the same apparatus as that employed for the catalytic study (pulse technique) (*6*). The analysis of the reaction products was performed by gas chromatography. The presence of CO_2, C_3H_4O, and H_2O was detected starting from 350°C. After cooling to room temperature in the mixture stream, the specimens were sealed in a glass tube and introduced into the XPS system without exposure to the atmosphere.

The spectra were collected by the computer in a sequential manner: C(1*s*), Fe(2*p*), O(1*s*), V(2*p*), Mo(3*d*), and Bi(4*f*). Binding

TABLE 1

Bulk and Surface Composition of the Fresh $Bi_{1-x/3}\square_{x/3-y}Me_y(V_{1-x}Mo_{x-y}Fe_y)O_4$ Samples

Samples			Bulk composition				Surface composition			
x	*y*	Me	Bi	V	Mo	Fe	Bi	V	Mo	Fe
0.45	0.00		0.85	0.55	0.45	—	1.04	0.37	0.66	—
0.60	0.00		0.80	0.40	0.60	—	0.84	0.34	0.93	—
0.45	0.15	Fe	0.85	0.55	0.30	0.30	0.70	0.32	0.56	0.33
0.60	0.15	Fe	0.80	0.40	0.45	0.30	0.87	0.30	0.68	0.25
0.45	0.15	Bi	1.00	0.55	0.30	0.15	1.10	0.43	0.44	0.20
0.60	0.20	Bi	1.00	0.40	0.40	0.20	1.17	0.29	0.51	0.20

energies, BE, were referenced to O(1*s*) at 530.5 eV, since the C(1*s*) signal was barely detectable. Data analysis procedure involved the following steps ((a) → (d)) for all the spectra: (a) smoothing; (b) inelastic background removal by a nonlinear "S-type" integral background profile; (c) curve-fitting using a mixed Gaussian–Lorentzian function by a least-squares method (*8*), and a procedure whereby the relative intensity and separation of the spin-orbit doublets were always fixed, whereas linewidths were either fixed at a constant value or allowed to vary and thus optimized by the program; and (d) determination of peak areas by integration of the appropriate peak, after steps (a) and (b) above. Surface composition was obtained from peak area ratios by using the elemental sensitivity factor method (*9*). This method takes into account some of the major factors influencing the experimental sensitivity, i.e., the electron escape depth and the detection efficiency of the energy analyzer. However, other factors are neglected, mainly the combined matrix and contamination effect on the attenuation length. The sensitivity factors were experimentally determined with a spectrometer of transmission characteristic equal to that used in this study and the following values were used: O(1*s*) = 0.61; V(2*p*) = 2.4; Fe(2*p*) = 4.6; Bi(4*f*) = 6.2; Mo(3*d*) = 2.5 (*10*). In addition to these procedures a satellite subtraction, namely $K\alpha_{3,4}$ components, was performed on the spectra obtained with Mg radiation. This subtraction was particularly important for the O(1*s*)–V(2*p*) region with the contribution of the α_3 and α_4 spectral lines of oxygen lying between the V($2p_{3/2}$) and V($2p_{1/2}$) photoemission peaks.

RESULTS

A. Fresh Samples

Iron-free samples ($x = 0.45$, $y = 0.00$; $x = 0.60$, $y = 0.00$) and iron-containing samples, both with Me = Fe ($x = 0.45$, $y = 0.15$; $x = 0.60$, $y = 0.15$) and Me = Bi ($x = 0.45$, $y = 0.15$; $x = 0.60$, $y = 0.20$) were examined "as prepared." The BE values determined are in agreement with literature data and consistent with the presence of Mo(VI) (Mo $3d_{5/2}$, 232.5 eV), Bi(III) (Bi $4f_{7/2}$, 159.9 eV), V(V) (V $2p_{3/2}$, 517.5 eV) and Fe(III) (Fe $2p_{3/2}$, 711.6 eV) (*11–14*). The iron-free samples exhibit FWHM values significantly larger (about 0.7 eV) than the corresponding values detected on the iron-containing samples. The O(1*s*) feature shows a low-intensity component at about 2 eV higher BE, due to the presence of chemisorbed hydroxyl species. Fe(2*p*) signals were similar in shape and position for all the iron-containing samples. Although the iron is present in different site symmetry in the Me = Fe series, namely, tetrahedral and eight-coordinated, a distinction between the ions in the different sites is not possible from the core level spectra, in line with the preceding observations regarding ions in tetrahedral and octahedral sites (*14*). The surface composition was evaluated from the $I(\text{Me})/I(\text{O}^{2-})$ intensity ratios, as described in the previous section. Table 1 compares the bulk composition obtained by chemical analysis with the surface composition derived from XPS measurements. All the samples show a surface enrichment in molybdenum and a lower vanadium surface concentration. Bismuth and iron surface composition similar to that of the bulk is found for all the samples. Moreover, the iron-free sample ($x = 0.45$, $y = 0.00$) exhibits a higher bismuth concentration than that of the bulk.

B. Hydrogen Reduced Samples

The reduction behaviour of samples with composition $x = 0.45$, $y = 0.00$; $x = 0.45$, $y = 0.15$ (Me = Fe); and $x = 0.45$, $y = 0.15$ (Me = Bi) was examined as a function of temperature by successively increasing the reduction temperature after each XPS measurement.

With the iron-free sample no changes either in BE or peak shape of bismuth, molybdenum, and vanadium are observed up

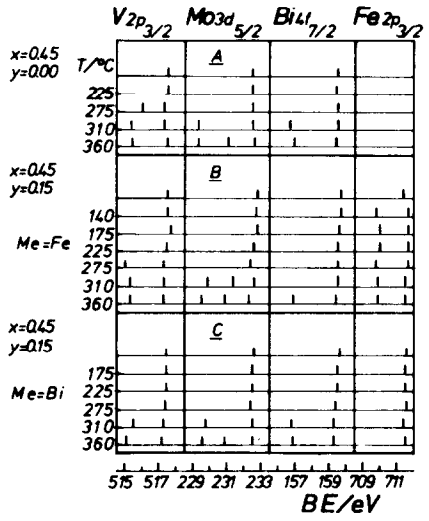

FIG. 1. Diagram of the BE values obtained before and after thermal treatment in flowing hydrogen in the XPS preparation chamber: (A) $x = 0.45$, $y = 0.00$ (iron-free sample); (B) $x = 0.45$, $y = 0.15$ (Me = Fe); (C) $x = 0.45$, $y = 0.15$ (Me = Bi).

to 225°C (Fig. 1A). On exposing the sample to hydrogen at 275°C, the V(2*p*) region shows a new component at 516.5 eV, due to V(IV) (*13*). For higher temperatures, 310° and 360°C, partial reduction of Mo(VI) to Mo(V) and Mo(IV), Bi(III) to Bi(0), and V(V) to V(III) is observed (Fig. 1A). An example of the V(2*p*), Mo(3*d*), and Bi(4*f*) XPS spectra before and after H_2 treatment is given in Fig. 2.

Fig. 1B summarizes the BE results for the iron-containing samples of composition Me = Fe. Starting from 275°C the V(2*p*) region shows a broadening on the low BE side of the spectrum. By curve-fitting the V(2*p*) feature is resolved as two components at 517.3 and 515.0 eV due to V(V) and V(III), respectively. After treatments at 310°C, and more markedly at 360°C, the Mo(3*d*) and Bi(4*f*) spectra indicate partial reduction. The new peaks in the Mo(3*d*) spectrum are ascribable to Mo(V) and to Mo(IV). The Bi(4*f*) component at 157.0 eV is attributed to Bi metal. The Fe(2*p*) region,

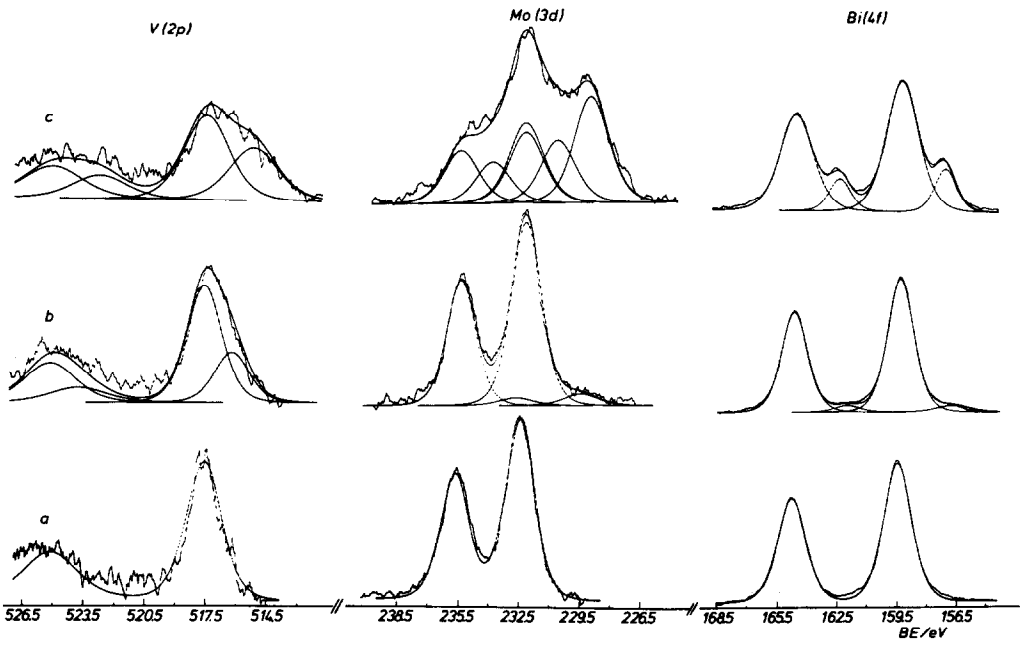

FIG. 2. XPS spectra for the $x = 0.45$, $y = 0.00$ sample. V(2*p*): (a) fresh sample; (b) 275°C, H_2; (c) 360°C, H_2. Mo(3*d*): (a) fresh sample; (b) 310°C, H_2; (c) 360°C, H_2. Bi(4*f*): (a) fresh sample; (b) 310°C, H_2; (c) 360°C, H_2. The intensity is 10^3 cps except for that of bismuth which is 5×10^3 cps.

by contrast, is already modified after treatment at 140°C for 30 min. By applying a spectral subtraction routine, beside the peak at 711.6 eV due to Fe(III), a new component at 709.8 eV becomes evident (Fig. 3, curve c). This feature, attributed to Fe(II), increases in intensity with the temperature.

The results obtained after H_2 treatments on the Me = Bi sample, containing iron in tetrahedral sites only, indicate constant BE values of Bi, V, Mo, and Fe up to 275°C (Fig. 1C). H_2 treatment at 310°C leads to partial reduction of V(V) to V(III), Mo(VI) to Mo(IV), and Bi(III) to Bi(0), which are manifested by the appearance of new components at 515.5, 229.9, and 156.8 eV, respectively. After treatment at 360°C the presence of Mo(V) is also detected. The Fe(2*p*) spectra recorded on this sample, both before and after H_2 treatments, were broad and of low intensity (Fig. 4). Hence the spectral subtraction procedure does not show clearly the presence of reduced iron species. However, a careful analysis of the peak profile for samples treated at 275°C or above shows a shoulder toward the low BE side and the lack of the shake-up signal associated with Fe(III) species (Fig. 4, curve b). The apparent lack of the satellite structure in the spectra can in fact result from a superimposition of Fe(II)- and Fe(III)-associated satellite intensity. Hydrogen treatments performed by increasing the temperature in steps and keeping it constant for a specified time (30 min, 1 h, 2 h), on a more concentrated iron sample ($x = 0.60$, $y = 0.20$) show that Fe(III) reduces after treatment at 225°C for 30 min. By spectral subtraction a component at 709.8 eV is apparent, the intensity of which increases as a function of time. The extent of reduction of molybdenum and vanadium, evaluated from the ratio of the peak area of the reduced species to the total signal area, was similar for all the samples and equal to 0.40 and 0.42, respectively. The iron-containing samples, both Me = Fe and Me = Bi, show a bismuth reducibility (0.35) higher than that of the iron-free sample (0.15).

For all the samples, on increasing the reduction temperature, the O(1*s*) signals be-

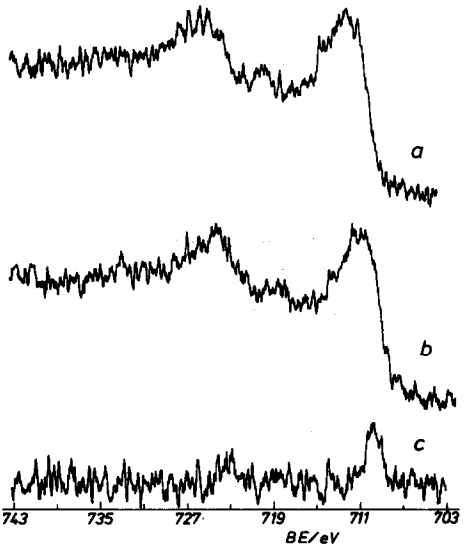

FIG. 3. Fe(2*p*) region, after smoothing, for the Me = Fe sample: (a) fresh sample; (b) 140°C, H_2; (c) after subtraction of spectrum (a) from spectrum (b).

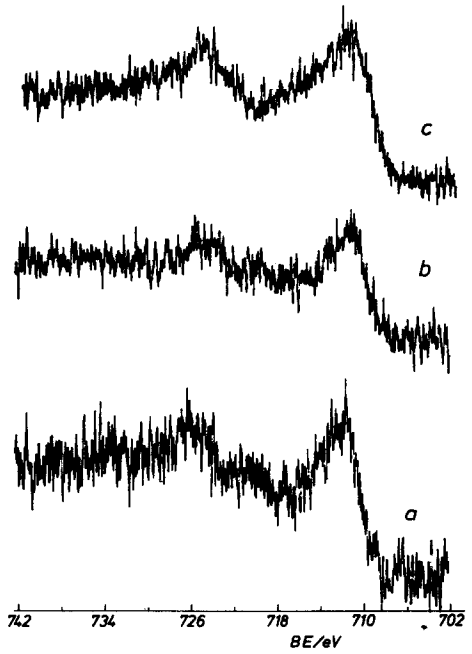

FIG. 4. Fe(2*p*) region, after smoothing, for the Me = Bi sample: (a) fresh sample; (b) 275°C, H_2; (c) 360°C, H_2.

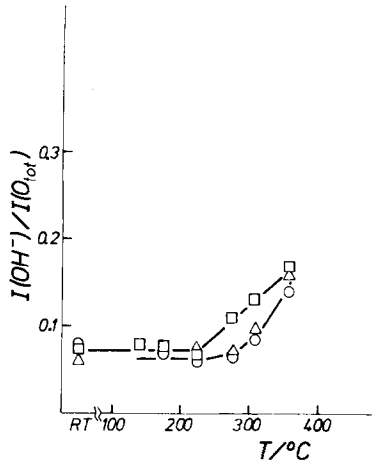

FIG. 5. $I(OH^-)/I(O_{tot})$ intensity ratios vs the temperature of treatment in flowing hydrogen: (○) $x = 0.45$, $y = 0.00$; (□) $x = 0.45$, $y = 0.15$ (Me = Fe); (△) $x = 0.45$, $y = 0.15$ (Me = Bi).

come composite with shoulders at 2 eV higher BE due to hydroxyl groups formed during the hydrogen treatments. In Fig. 5 the variation of the $I(OH)/I(O_{tot})$ intensity ratios as a function of the temperature is shown. From Fig. 5 it can be seen that the intensity ratios increase with increasing temperature.

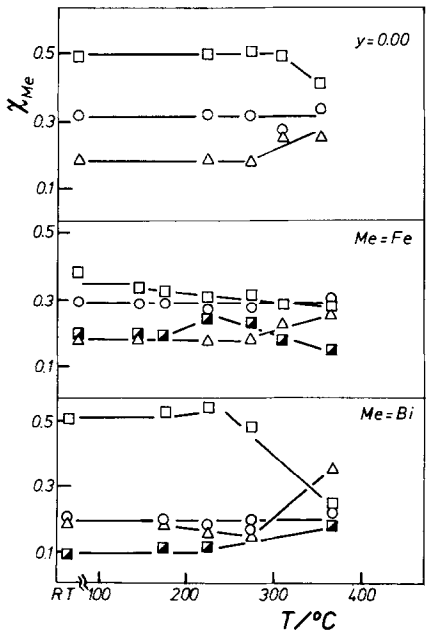

FIG. 6. Variation in the surface composition, as cation mole fraction, χ_{Me}, against the temperature of treatment in hydrogen for samples with or without iron: (□) Bi; (○) Mo; (△) V; (◪) Fe.

The variation of the surface composition, as cation mole fraction, χ_{Me}, plotted against the H_2 treatment temperature, is reported in Fig. 6. For the iron-free sample ($y = 0.00$), the reduction process occurs with a surface enrichment in vanadium and a concomitant decrease in bismuth, the molybdenum concentration being practically unchanged. For the iron-containing sample, Me = Fe, reduction leads to slight vanadium surface enrichment with a parallel decrease in bismuth and iron. The Me = Bi samples become progressively enriched in vanadium with a decrease in the bismuth surface content. A slight enrichment is detected for iron. Also for both Me = Fe and Me = Bi samples the reduction treatments do not affect the molybdenum surface concentration.

C. Propene Treatments

Figure 7 summarizes the BE values obtained before and after propene treatments in the temperature range 140–360°C on the iron-free sample ($x = 0.45$, $y = 0.00$) (Fig. 7A) and on both the iron-containing samples Me = Fe ($x = 0.45$, $y = 0.15$) (Fig. 7B) and Me = Bi ($x = 0.60$, $y = 0.20$) (Fig. 7C). At 140°C the Bi(4*f*) region indicates partial reduction for all the samples investigated. Bi(0) at 156.8 eV is present in the iron-free and the iron-containing Me = Bi samples (Fig. 7A and 7C). The Me = Fe sample (Fig. 7B) shows at 140°C a component at 158.0 eV attributable to Bi(I) (*15*). However, starting from 175°C a Bi(0) contribution is always present.

As for the V and Mo peaks in the iron-free sample, the treatment at 275°C reveals the incipient reduction of V(V) to V(III), while Mo(V) appears at a higher temperature. For the iron-containing samples the reduction of Mo(VI) to Mo(V) and V(V) to V(III) is achieved only after treatment at 360°C for 30 min.

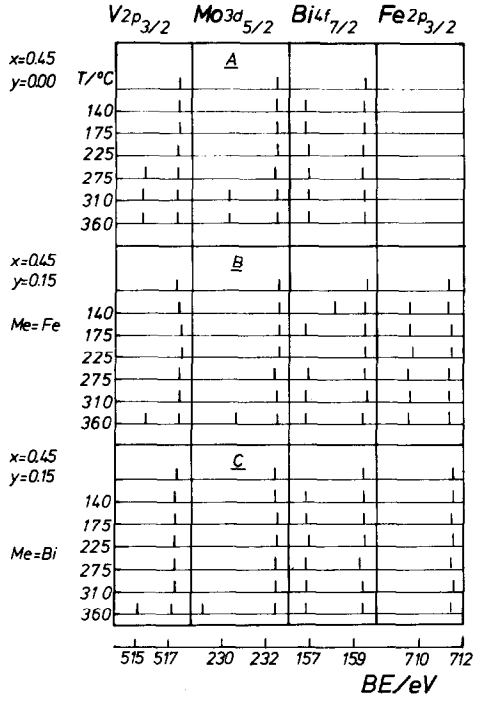

FIG. 7. Diagram of the BE values before and after propene treatment: (A) $x = 0.45$, $y = 0.00$; (B) $x = 0.45$, $y = 0.15$ (Me = Fe); (C) $x = 0.60$, $y = 0.20$ (Me = Bi).

Fe(II) was clearly detected at 140°C by spectral subtraction in the Me = Fe sample, while no clear evidence of iron reduction could be obtained on the Me = Bi specimen.

An evaluation of the extent of reduction for each different element has been made through the ratio of the reduced species peak area to the total signal area of a given element. The vanadium degree of reduction is found to increase with the temperature for the iron-free sample, while the iron-containing specimens (both Me = Bi and Me = Fe) show a very low reduction extent. For all the samples the molybdenum reducibility is small, whereas the extent of reduction of bismuth shows a different trend. For the Me = Bi and Me = Fe samples the Bi(O)/Bi(tot) ratio is low and slightly increases over the whole temperature range; for the iron-free sample the bismuth degree of reduction is found to decrease by increasing the temperature, reaching a constant value from 275°C.

The O(1*s*) signal is also modified by the propene treatments. Starting from 140°C the O(1*s*) signals become composite, with a component at about 2 eV higher BE. For all the specimens, starting at 175°C, the O(1*s*) signal becomes composite with a component at about 2 eV higher BE, the intensity of which increases in the temperature ranges 225–310°C and then is removed completely after treatment at 360°C. This component can be assigned to surface hydroxyl groups or water formed during the propene treatments, since this peak is not accompanied by the appearance of additional C(1*s*) signals. The presence of oxygenated hydrocarbon species bonded to the surface can therefore be neglected.

The variation of the surface composition, as cation mole fraction, χ_{Me}, is illustrated in Fig. 8. The propene treatment leads to a strong bismuth surface enrichment for all the samples investigated, while the surface concentration of all other elements remains practically unchanged.

D. Propene + Oxygen Mixture Treatments

The BE results obtained after treatment with the flowing reacting mixture $C_3H_6 : O_2 : He$ are summarized in Table 2. In Table 2 the FWHM values are also listed within parentheses.

For all the samples, the V(2*p*) signals show a broadening in the temperature range 200–400°C, whereas in the Bi(4*f*) feature a tail on the low BE side is present over the whole temperature range examined. This contribution can be assigned to bismuth metal. The Mo(3*d*) region remains unchanged for the iron-free ($x = 0.60$, $y = 0.00$) and iron-containing Me = Fe sample, while the Me = Bi sample shows a broadening in the range 200–250°C. In addition, for the Me = Fe specimen, by spectral subtraction, a small contribution due to Fe(II) is obtained in all the spectra. The O(1*s*) fea-

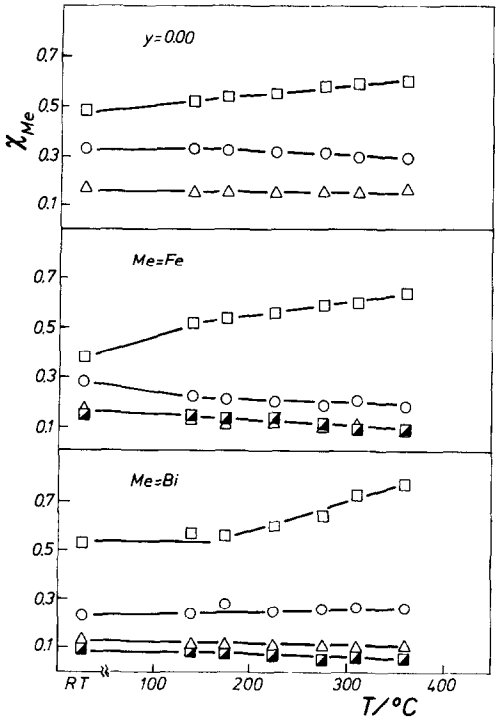

FIG. 8. Variation in the surface composition, as cation mole fraction, χ_{Me}, as a function of the temperature of treatment in flowing propene for iron-free ($x = 0.45$, $y = 0.00$) and iron-containing ($x = 0.45$, $y = 0.15$) Me = Fe and ($x = 0.60$, $y = 0.20$) Me = Bi specimens: (□) Bi; (○) Mo; (△) V; (◪) Fe.

ture remains unchanged with respect to the untreated samples.

For all the specimens no variation in surface composition has been detected after propene + oxygen exposure in the whole temperature range examined.

DISCUSSION

The experimental results show that distinct changes occur in the surface structure both as regards the chemical state and the surface composition.

The XRD analysis data obtained on "fresh samples" show that all the samples are monophasic with the scheelite tetragonal structure (*5*). Nevertheless, the XPS data indicate that the surface composition is slightly different from that of the bulk deduced by chemical analysis, as shown in Table 1.

On exposure of the samples to H_2, different reduction behaviour was observed depending on the chemical composition. The iron-containing specimens are reduced at low temperature. The reduction behaviour of the surface is in agreement with a previous investigation performed by other methods on the reduction of bismuth molybdovanadates with or without iron (*7*). In particular, optical absorbance and magnetic measurements in flowing hydrogen reveal that on the samples with iron a significant reduction takes place from 250°C, whereas for the samples without iron a comparable degree of reduction is reached only at 400°C.

The reduction process occurs with the formation and the retention of hydroxyl groups at the catalyst surface (Fig. 5). This behaviour is in agreement with TG experiments (*7*) which show no significant weight loss up to ~300 and ~400°C for iron-containing and iron-free samples, respectively. The reduction process also has a pronounced influence on the surface composition. The decrease in surface bismuth concentration observed for all the samples (Fig. 6) can be explained by the reduction of Bi(III) to bismuth metal: the decrease in intensity arises from the sintering of the reduced bismuth due to its low melting point of 270°C. This view is supported by the detection of large metal particles of bismuth as revealed by XRD analysis performed on samples treated at 360°C for 30 min in the XPS apparatus.

The surface enrichment of vanadium could be due to two distinct factors, namely, uncovering of oxidic components from sintering of metal bismuth and/or surface migration of the suboxides formed during reduction. The considerable change in the surface composition found for the iron-free and Me = Bi samples indicates that the reduction is localized in the vicinity of the surface layers. Moreover, the presence in the Me = Fe samples of iron in both the tetrahedral and eight-coordinated sites of the scheelite structure, on the other hand,

TABLE 2

BE and FWHM Values[a] for $Bi_{1-x/3}\square_{x/3-y}Me_y(V_{1-x}Mo_{x-y}Fe_y)O_4$ Samples after Treatments with the Reacting Mixture $C_3H_6 + O_2$ in He Stream

Sample	T (°C)	V $2p_{3/2}$ (eV)	Mo $3d_{5/2}$ (eV)	Bi $4f_{7/2}$ (eV)	Fe $2p_{3/2}$ (eV)
$x = 0.60$, $y = 0.00$		517.4(2.42)	232.5(2.26)	159.5(2.24)	—
	200	517.2(2.28)	232.6(2.32)	159.5(2.37)	—
				157.2[b]	
	350	517.4(2.98)	232.5(2.44)	159.4(2.50)	—
				157.2[b]	
	400	517.5(2.93)	232.5(2.36)	159.5(2.32)	—
				157.1[b]	
	450	517.5(2.39)	232.6(2.34)	159.6(2.22)	—
				157.1[b]	
$x = 0.45$, $y = 0.15$		517.5(1.70)	232.6(1.50)	159.4(1.70)	711.5
(Me = Fe)	200	517.5(2.20)	232.7(1.73)	159.7(1.63)	711.5
	250	517.3(2.10)	232.5(1.73)	159.5(1.67)	711.6
				156.9[b]	709.9[c]
	350	517.3(2.10)	232.5(1.70)	159.5(1.70)	711.5
				156.8[b]	709.8[c]
	400	517.4(2.10)	232.6(1.66)	159.7(1.70)	711.6
				156.8[b]	709.9[c]
$x = 0.45$, $y = 0.15$		517.5(1.70)	232.5(1.50)	159.6(1.70)	711.6
(Me = Bi)	200	517.5(2.34)	232.5(2.11)	159.5(2.18)	711.5
	250	517.3(2.20)	232.5(2.22)	159.5(1.80)	711.5
				156.9[b]	
	350	517.2(2.25)	232.5(1.80)	159.4(1.70)	711.5
				156.9[b]	
	450	517.4(1.89)	232.5(1.70)	159.5(1.70)	711.4
				156.8[b]	

[a] Within parentheses.
[b] Tail.
[c] From spectra subtraction.

stabilizes the catalyst against extensive variation in the surface composition, probably enhancing the mobility of the lattice oxygen ions.

Analysis of the XPS spectra after propene treatment reveals two main features, regardless of the sample composition: (i) the reduction of bismuth at low temperature (Fig. 7), and (ii) an increase in its intensity over the whole temperature range examined (Fig. 8). Bismuth is already reduced to Bi(0) at 175°C for all the samples, while for the Me = Fe specimen the intermediate formation of lower bismuth oxide, such as Bi(I), is also detected at 140°C. Reduction of molybdenum and vanadium is achieved only at high temperature. The bismuth surface enrichment can be accounted for by the preferential reactivity of bismuth with ensuing migration to the surface and reduction. The preferential bismuth migration to the surface is shown for the oxidized species. In fact the relative ratios $I(Bi^{III})/I(O^{2-})$ and $I(Bi^0)/I(O^{2-})$ (Fig. 9) show that the $I(Bi^{III})/I(O^{2-})$ intensity ratios increase for all the specimens investigated over the whole temperature range examined, while the $I(Bi^0)/I(O^{2-})$ intensity ratios indicate a low and slight increase in the metal formation for the Me = Fe and Me = Bi samples

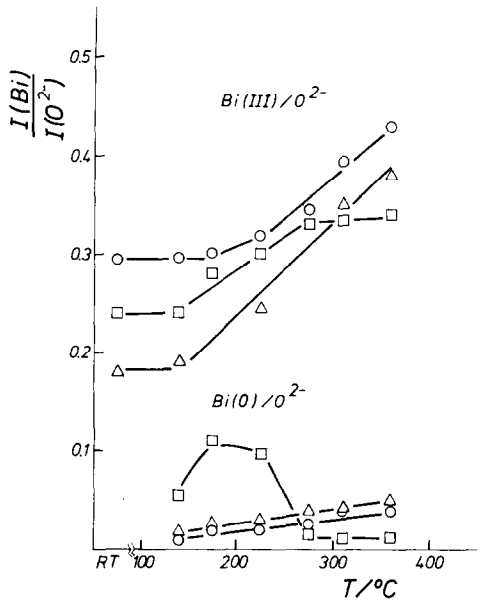

FIG. 9. $I(Bi)/I(O^{2-})$ intensity ratios vs the treatment temperature in flowing propene: (□) $x = 0.45$, $y = 0.00$; (△) $x = 0.45$, $y = 0.15$ (Me = Fe); (○) $x = 0.60$, $y = 0.20$ (Me = Bi).

and a higher metal formation in the range 140–225°C for the iron-free sample. It must be recalled that this specimen shows a bismuth surface enrichment so that the high degree of metal formation can be due to the reduction of bismuth to metal present in the outer layer, which aggregates at temperatures higher than the bismuth melting point (270°C).

The results obtained in the present investigation support the hypothesis of a strong Bi^{3+}–olefin bond, as proposed by Haber (*16*) for catalysts like molybdates and tungstates in the olefin oxidation reactions. It has also been found that the propene reacts directly with bismuth oxide to give C_6 olefinic products, with reduction of Bi_2O_3 to metal (*17*).

The results obtained under conditions leading to the catalytic oxidation of propene indicate that the surfaces of the catalysts remain extensively oxidized and that the surface compositions reflect those found for the untreated samples. The XPS line broadening observed for the vanadium and molybdenum by increasing the temperature of sample treatment could be due to incipient reduction of these species.

A final comment concerns the results of the present investigation and the catalytic properties for propene oxidation of the same samples as reported in a previous study (*6*). In both the $x = 0.45$ and the $x = 0.60$ series the catalytic behaviour was found to depend on the compositional parameter y and on whether Me = Fe or Me = Bi. Both rate constant and selectivity were indeed higher for catalysts with $y = 0$ (presence of cation vacancies), and in most cases for catalysts $y = x/3$, Me = Fe in comparison with catalysts $y = x/3$, Me = Bi (absence of cation vacancies in both samples). These differences cannot be accounted for by a different reducibility of surface Bi^{3+} ions, since a low BE component of the Bi(4*f*) peak is present in all the catalysts reduced with propene at a temperature as low as 140°C (see Fig. 6).

A possible explanation can be found by considering that the mobility of the oxygen ions might be considerably different among the samples examined. In fact in a recent study Ueda *et al.* (*18*) pointed out that the bulk diffusion of O^{2-} ions in scheelite catalysts is indirectly related to the introduction of disordered cation vacancies. The consequent formation of distorted tetrahedra-sharing oxygen ions would make the diffusion of oxygen ions easier between bulk and surface. Samples with $y = 0$ should, therefore, possess higher mobility for the anions, while the samples with $y = x/3$ should have lower O^{2-} mobility, since no cation vacancies are present. Moreover, a study of the redox properties of these catalysts using pulses of 1-butene and pulses of oxygen (*19*) clearly indicated that in the samples with $y = x/3$, Me = Fe bulk oxygen diffusion is faster than in the samples with $y = x/3$, Me = Bi. It can therefore be suggested that the reduction actually involves different depths for the various catalysts. The easier the diffusion of O^{2-} ions from the bulk to the surface, the higher the number

of subsurface layers involved. XPS cannot discriminate whether a minimum depth has been involved in the reduction in every case, but the catalytic properties may be quite different, since it is generally accepted that a high mobility of oxygen ions in these catalytic systems is required in order to restore the adsorption site and to maintain the overall catalytic process. Moreover, the high mobility of the lattice oxygen ions can also be responsible for the apparent stability of these and similar systems under catalytic conditions.

ACKNOWLEDGMENTS

This work was supported by CNR, "Progetto Finalizzato Chimica Fine e Secondaria." The authors thank Professor A. Cimino for critically reading the manuscript.

REFERENCES

1. (a) Keulks, G. W., Krenzke, L. D., and Notermann, T. N., *in* "Advances in Catalysis" (D. D. Eley, H. Pines, and P. B. Weisz, Eds.), Vol. 27, p. 183. Academic Press, New York, 1978. (b) Grasselli, R. K., and Burrington, J. D., *in* "Advances in Catalysis" (D. D. Eley, H. Pines, and P. B. Weisz, Eds.), Vol. 31, p. 133. Academic Press, New York, 1981. (c) Grasselli, R. K., and Burrington, J. D., *Ind. Eng. Chem. Prod. Res. Dev.* **23,** 393 (1984).
2. Sleight, A. W., *in* "Advanced Materials in Catalysis" (J. J. Burton and R. L. Garten, Eds.), p. 181. Academic Press, New York, 1977.
3. Brückman, K., Haber, J., and Wiltowski, T., *J. Catal.* **106,** 188 (1987).
4. Grasselli, R. K., *Appl. Catal.* **15,** 127 (1985).
5. Porta, P., Lo Jacono, M., Valigi, M., Minelli, G., Anichini, A., De Rossi, S., and Gazzoli, D., *J. Catal.* **100,** 86 (1986).
6. De Rossi, S., Lo Jacono, M., Porta, P., Valigi, M., Gazzoli, D., Minelli, G., and Anichini, A., *J. Catal.* **100,** 95 (1986).
7. Valigi, M., De Rossi, S., Gazzoli, D., and Porta, P., *Gazz. Chim. Ital.* **116,** 97 (1986).
8. Maddams, W. F., *Appl. Spectrosc.* **34,** 245 (1980).
9. Wagner, C. D., Davis, L. E., Zeller, M. V., Taylor, J. A., Raymond, R. H., and Gale, L. H., *Surf. Interface Anal.* **3,** 211 (1981).
10. Berresheim, K., private communication.
11. Morgan, W. E., Stec, W. J., and Van Wazer, J. R., *Inorg. Chem.* **12,** 953 (1973).
12. Grzybowska, B., Haber, J., Marczewski, W., and Ungier, L., *J. Catal.* **42,** 327 (1976).
13. Sawatzki, C. A., and Post, D., *Phys. Rev. B* **20,** 1546 (1979).
14. Wandelt, K., *Surf. Sci. Rep.* **2,** 1 (1981).
15. Okamoto, Y., Morikawa, F., Degawa, J., Imanaka, T., and Teranishi, S., *Chem. Lett.*, 1853 (1983).
16. Haber, J., *Int. Chem. Eng.* **15,** 21 (1975).
17. Massoth, F. E., and Scarpiello, D. A., *J. Catal.* **21,** 225 (1971), and references therein.
18. Ueda, W., Chen, C. L., Asakawa, K., Moro-oka, Y., and Ikawa, T., *J. Catal.* **101,** 360 (1986), and references therein.
19. De Rossi, S., to be published.